

Just Say the Word: Annotation-Free Fine-Grained Object Counting

Adriano D’Alessandro

Ali Mahdavi-Amiri

Ghassan Hamarneh

Simon Fraser University

{acdaless, amahdavi, hamarneh}@sfu.ca

Abstract

Fine-grained object counting remains a major challenge for class-agnostic counting models, which overcount visually similar but incorrect instances (e.g., jalapeño vs. poblano). Addressing this by annotating new data and fully retraining the model is time-consuming and does not guarantee generalization to additional novel categories at test time. Instead, we propose an alternative paradigm: Given a category name, tune a compact concept embedding derived from the prompt using synthetic images and pseudo-labels generated by a text-to-image diffusion model. This embedding conditions a specialization module that refines raw overcounts from any frozen counter into accurate, category-specific estimates—without requiring real images or human annotations. We validate our approach on LOOKALIKES, a challenging new benchmark containing 1,037 images across 27 fine-grained subcategories, and show substantial improvements over strong baselines. Code and data will be released upon acceptance.

1. Introduction

Class-agnostic counting (CAC) models reduce the annotation burden by allowing users to specify object categories at inference time [10, 26, 35]. This is achieved by conditioning the image features on text or visual exemplars. While these models perform well on broad categories, they struggle in more challenging fine-grained scenarios by overcounting any objects that *look* visually similar to the specified object (see Fig. 1). This limits their applicability to many real-world tasks like ecological surveying, inventory tracking, and agritech, where distinguishing subtle visual differences is essential.

A natural response to the failure of class-agnostic counters in fine-grained settings is to manually collect labeled examples for several subcategories. However, this approach is not only excessively time-consuming—it fails to address the deeper challenge of generalizing to unseen fine-grained



Figure 1. Many class-agnostic counting methods incorrectly count all visually similar objects.

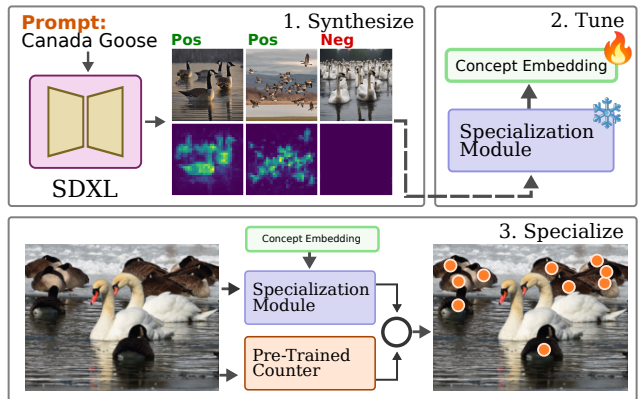


Figure 2. Given *only* a text prompt, our method adapts counting models to novel fine-grained categories at test-time.

categories at inference time. Prior work has shown that CAC models struggle to generalize even between the broad categories in datasets like FSC-147 and FSCD-LVIS [5] let alone to subtle intra-class variations. In this context, conditioning on visual exemplars or text at inference time becomes a limitation, as these methods fail to distinguish previously unseen, visually similar instances.

To overcome this limitation, we propose a more effective approach: using synthetic data to fine-tune prompts for each category instead of relying on fixed conditioning (Fig. 2).

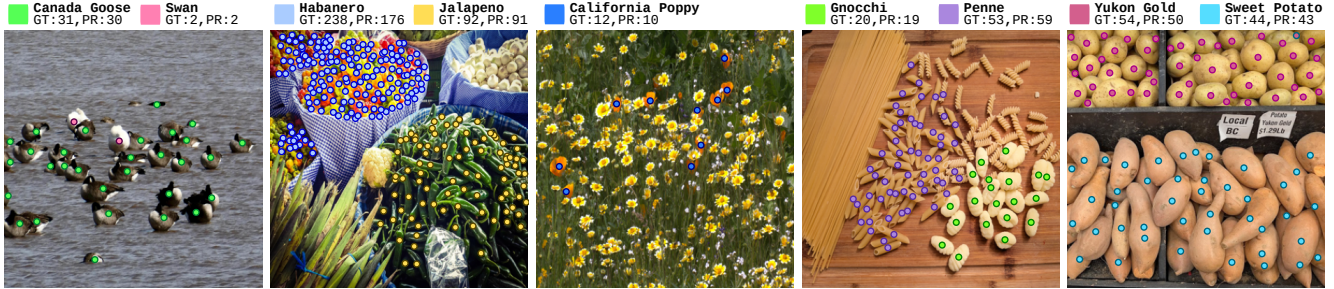


Figure 3. Our method accurately counts fine-grained target categories while suppressing visually similar distractors in the complex and cluttered scenes of the LOOKALIKES dataset. The base model used is PSeCO, with categories indicating the intended target of the concept vector. GT denotes the ground truth count, and PR indicates our method’s prediction.

Inspired by recent advances in prompt tuning for vision and language models [12, 13, 34], we propose a method to adapt a pre-existing counting model to novel categories using synthetic data by tuning only a *concept embedding*, which is a compact, category-specific representation that distinguishes the target object from visually similar distractors.

Our approach builds on two key insights. First, class-agnostic counters tend to have high recall but low precision in fine-grained scenes—they produce many false positives, but few false negatives. Thus, filtering out these false positives can significantly improve accuracy. Second, we observe that latent diffusion models such as SDXL can generate realistic fine-grained images from text, providing a rich source of visual information for learning novel concepts.

Given only a category name (e.g., California poppy), our approach uses a text-to-image diffusion model to synthesize images and extract the cross-attention maps between the prompt and image features during generation. These attention maps are converted into coarse pseudo-segmentation masks that localize the named category (see: synthesis step in Fig. 2). For our specialization module, we modify a frozen open-vocabulary segmentation model by conditioning it on concept embeddings. This module can be rapidly adapted to a new category by prompt-tuning the embedding on synthetic image-mask pairs (see the tuning step in Fig. 2). At inference time, the module is applied to the outputs of a frozen class-agnostic counter to suppress visually similar but incorrect objects, transforming noisy overcounts into clean, category-specific estimates.

To further ensure the exclusion of distractors, we incorporate hard negative supervision. We explore different strategies for selecting and synthesizing visually similar but incorrect categories and use them as the basis for a negative concept loss. This loss penalizes the guidance module when it activates on these hard negatives, pushing the concept embedding toward greater specificity. As shown in Fig. 3, our system accurately adapts to a novel fine-grained category on the fly without requiring any real images, annotations, or retraining of the counting model—just the category name.

Prior class-agnostic object counting benchmarks, such as FSC147 [26], focus on single broad categories (e.g., Boxes vs Apples) and lack highly specific fine-grained distinctions (e.g., Male Mallard Ducks vs Female Mallard Ducks). To address this, we introduce LOOKALIKES, a challenging fine-grained object counting dataset that focuses on related objects within a taxonomy. It spans 27 subcategories across 8 domains, ranging from bird species to pepper cultivars to pasta noodle shapes, and includes images containing multiple subcategories, reflecting the real-world challenge of distinguishing visually similar objects. Our method substantially outperforms strong zero-shot baselines, addressing a gap in the counting pipeline: from “count all the peppers” to “count only the habaneros.”

Finally, we conclude this work by ablating various aspects of the setup and evaluating the performance of multiple baselines on LOOKALIKES. In summary, our contributions are as follows:

- We propose a novel annotation-free counting method that adapts to new fine-grained object categories at test-time using synthetic data.
- Our method serves as a generic plug-in module that transforms CAC networks into fine-grained counters by learning category-specific concept embeddings at test time.
- We introduce LOOKALIKES, a new benchmark dataset designed to evaluate fine-grained counting performance and generalization across 27 subcategories.

2. Related Work

Class-Agnostic Counting. Few-shot counting was introduced with the FSC147 dataset [26], where methods use visual exemplars to define which objects to count in an image [4, 8, 23, 29]. Zero-shot counting [32, 33, 35] extends this paradigm by defining classes through text-based prompts,

removing the need for image exemplars and enabling flexible, text-driven counting. Additionally, unsupervised and weakly supervised methods [7,9,14,27] have been explored for single-category object counting.

Similar to our method, DAVE [23] introduced a strategy for reducing false positives. DAVE relies on spectral clustering, which fails entirely on fine-grained counting (See: Fig 4), despite its filtering mechanism. Instead, our approach learns category-specific specialization using synthetic data.

Learning from Synthetic Images. Synthetic image data generated by latent diffusion models is increasingly explored as a solution for real-world challenges [11, 25, 28]. Closest to our approach, AFreeCA [7] uses weak signals from synthetic images for single-category, unsupervised object counting. In contrast, our work extends this concept to multi-class fine-grained categories, using synthetic data to adapt pre-trained networks to fine-grained counting.

Fine-Grained Image Analysis. Taxonomy-based analysis, as seen in datasets like CUB-200 [30] and Oxford Flowers [22], categorizes images based on shared taxonomies with subtle inter-category differences. Our work extends taxonomy-based analysis to annotation-free object counting.

Attribute-based analysis focuses on identifying objects with *fine-grained attributes* like color or location [17, 18, 31]. Similar to our work, the REC-8K dataset [6] tackles referred-expression counting, allowing for distinctions between simple categories and attributes, such as color (e.g., *blue car vs. red car*). However, REC-8K’s training and test sets share significant category overlap (75%), focusing primarily on capturing novel attributes for established categories. In contrast, our work aims to extend to novel *fine-grained categories* without requiring any annotations, addressing a previously unexplored challenge.

Prompt Tuning. Prompt tuning is a parameter-efficient strategy that adapts large, frozen models by optimizing a small set of learned input tokens or embeddings [12, 34]. The authors in [13] introduced this approach for language models, showing that a small set of continuous vectors can steer model behavior without updating model weights. We extend this strategy to fine-grained dense counting by tun-



Figure 4. DAVE [23] uses a filtering strategy to reduce false positives but fails on fine-grained categories, leading to overcounting, as seen in these images of peppers

ing a concept embedding using synthetic data.

3. Lookalikes Dataset

To evaluate the ability of counting models to distinguish between visually similar object categories, we introduce the LOOKALIKES dataset, a novel taxonomy-based benchmark uniquely combining fine-grained recognition with multi-class counting. Unlike broad-category counting datasets, which identify all objects of a general type (e.g., “birds” or “peppers”), our dataset focuses on distinguishing between sibling subcategories within the taxonomy, such as apple cultivars or waterfowl species.

The Lookalikes dataset consists of 8 parent domains, designed to test counting models on differentiating similar objects in densely populated scenes (averaging 36.4 objects per image with a maximum of 656). These domains are: Apple cultivars, human roles, pasta varieties, pepper cultivars, potato cultivars, tomato cultivars, waterfowl species, and wildflower species. Each domain contains 2 to 6 sibling categories, and 83% of images have 2 or more siblings present within the image, with some images containing as many as 6 siblings (see: Tab 1). The dataset also includes images with additional, infrequently occurring subcategories labeled as “other”. These less common subcategories are grouped together and treated as a single distractor class.

Overall, LOOKALIKES addresses a critical gap and serves as a benchmark for evaluating fine-grained object counting in high-density images with multiple subcategories from the same taxonomy, challenging models to distinguish inter-class variations within densely populated scenes. Sample images in Fig. 5 illustrate the dataset’s complexity, making LOOKALIKES a valuable resource for assessing a model’s ability to generalize to fine-grained object categories.

3.1. Dataset Split and Evaluation

For easier access, we structure Lookalikes as a test-set only dataset with a structure similar to the test split of the FSC147 dataset [26]. Whereas the FSC147 test-set contains 1,190 images across 29 broad categories, Lookalikes contains 1,037 images across 8 parent categories and 27 subcategories. This setup focuses on evaluating models trained without manual annotations from fine-grained categories, assessing their ability to generalize to unseen classes.

# Subcategories	1	2	3	4	5	6
# Images	182	600	164	58	29	4

Table 1. Distribution of subcategories per image. Most images contain 2 or more subcategories.



Figure 5. Sample images from LOOKALIKES, our fine-grained counting dataset. The dataset includes crowded, diverse images with multiple distinct object subcategories in each scene, highlighting the variety and complexity of the data.

3.2. Data Collection and Annotation Process

To construct the LOOKALIKES dataset, we collected images under Creative Commons licenses from Flickr, Unsplash, and Pexels, using targeted search queries based on each object’s subcategory name. Selection criteria focused on maintaining crowd density, visual variability, and the presence of multiple subcategories within each image, creating realistic scenarios for fine-grained counting. For annotations, we provide the object counts along with point labels applied to the approximate center of each object within an image, with each label specifying the fine-grained category.

4. Methodology

We propose a prompt tuning strategy that tunes subcategory-specific concept embeddings for a category specialization module using only synthetic supervision. Given only a category name, we generate synthetic images with a text-to-image diffusion model and extract coarse but semantically meaningful cross-attention maps (Fig. 6, Top). While noisy, these maps provide sufficient spatial guidance to tune new concept embeddings, enabling us to adapt existing counting models and substantially improve their performance in fine-grained settings (Fig. 6, Bottom).

The remainder of this section describes each component of our approach. We begin by outlining the generation of synthetic exemplars and attention maps, including strategies for selecting hard negative categories. We then explain how these are used to tune concept embeddings. Finally, we describe how the resulting specialization module is applied to refine the output of a frozen class-agnostic counting model.

4.1. Synthesize Step

Creating annotated data for fine-grained categories requires considerable manual effort, making it impractical at scale. To address this, we utilize Stable Diffusion XL (SDXL) [24] as a synthetic data generation tool as it is capable of representing many specific fine-grained cate-

gories and producing high-quality, realistic images containing multiple objects. This capability allows us to generate a diverse set of synthetic images that closely resemble real-world scenes. Our approach further leverages the internal cross-attention mechanism of SDXL to generate fine-grained attention annotations for these synthetic images:

$$(x^{\text{syn}}, \mathbf{A}_{\text{map}}^{\{\text{CLS}\}}) \leftarrow \text{SDXL}(\text{prompt}^{\{\text{CLS}\}}), \quad (1)$$

where x^{syn} is a synthetic image containing objects from category $\{\text{CLS}\}$, $\text{prompt}^{\{\text{CLS}\}}$ is a text prompt describing the objects, and $\mathbf{A}_{\text{map}}^{\{\text{CLS}\}}$ is a semantic attention heat map that localizes the objects in x^{syn} . As illustrated in Fig. 6, the process begins by tokenizing the prompt and generating embeddings for each token, which are then fed into SDXL’s cross-attention layers during generation. Our objective is to extract the cross-attention maps that capture the interactions between the synthetic image features and the specific token for the fine-grained category $\{\text{CLS}\}$.

We define the cross-attention map from SDXL layer l as

$$\mathbf{A}_l \in \mathbb{R}^{C \times H \times W \times Z}, \quad (2)$$

where C , H , W , and Z represent the channels, height, width, and token sequence length, respectively. We then use the $\{\text{CLS}\}$ token index to select the corresponding cross-attention map, denoted as:

$$\mathbf{A}_l^{\{\text{CLS}\}} \in \mathbb{R}^{C \times H \times W}. \quad (3)$$

If the category name contains multiple tokens, we select the index representing the token with the maximum value in \mathbf{A}_l .

To create a consolidated attention map for the $\{\text{CLS}\}$ token across a set of layers $L = \{l_1, l_2, \dots, l_n\}$, we first concatenate the attention maps from these layers:

$$\mathbf{A}_{\text{concat}}^{\{\text{CLS}\}} = [\mathbf{A}_{l_1}^{\{\text{CLS}\}}, \dots, \mathbf{A}_{l_n}^{\{\text{CLS}\}}] \in \mathbb{R}^{H \times W \times (n \cdot C)}. \quad (4)$$

We then compute the channel-wise mean to obtain a spatial

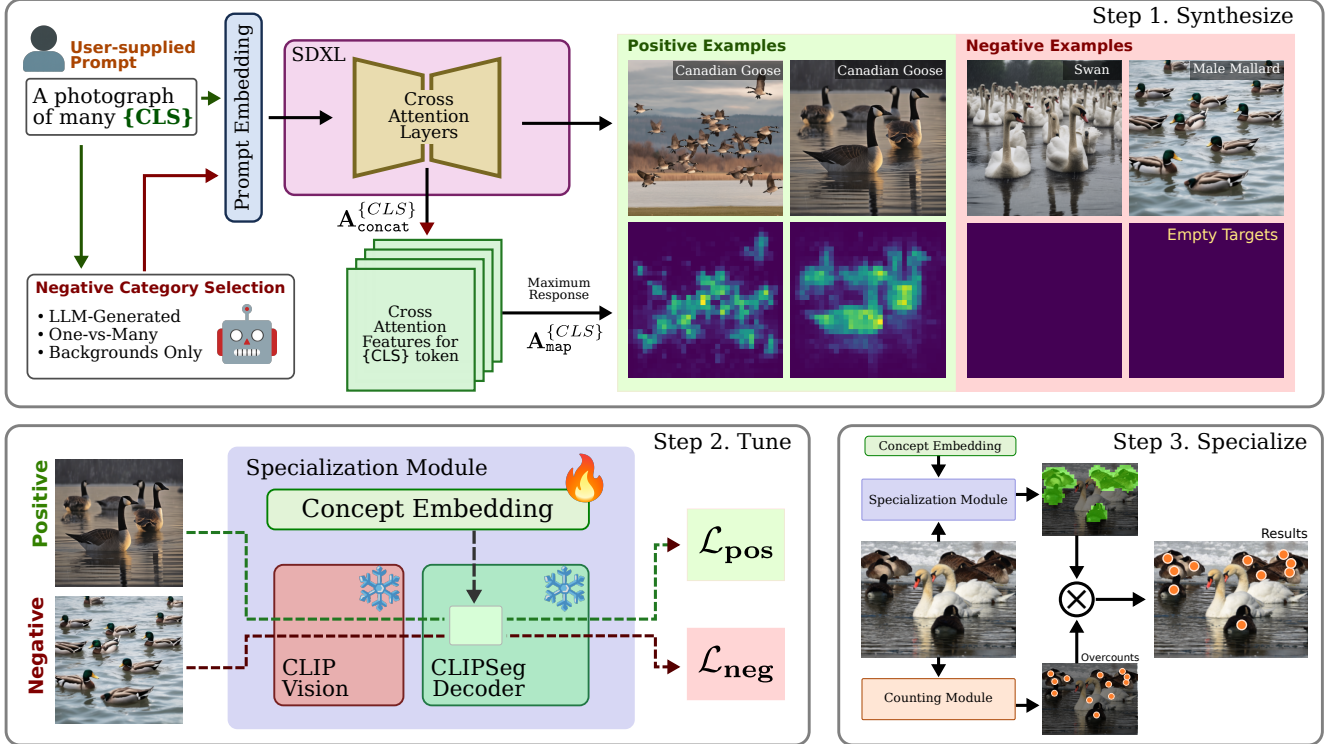


Figure 6. Given a category name $\{CLS\}$, our method proceeds in three stages: synthesize data with attention maps, tune a category-specific concept embedding using synthetic supervision, and then filter the output from a class-agnostic counter.

map that localizes the fine-grained objects:

$$\mathbf{A}_{\text{map}}^{\{CLS\}} = \frac{1}{n \cdot C} \sum_i^{n \cdot C} \mathbf{A}_{\text{concat}}^{\{CLS\}}[i]. \quad (5)$$

By extracting the cross-attention output for the relevant token and averaging across channels, we generate a spatial attention map that highlights the locations of objects within the fine-grained category. This setup yields a synthetic image x^{syn} , a fine-grained category label $y^{\{CLS\}}$, and an attention map $\mathbf{A}_{\text{map}}^{\{CLS\}}$ that localizes the fine-grained objects, providing a pseudo-annotation for each generated image.

4.1.1 Selecting Negative Categories

Images containing negative categories can help refine the concept embedding by encouraging it to suppress visually similar but incorrect categories. Given a set of negative category names, we synthesize images as before but assign an empty attention map to prevent the Specialization module from activating:

$$\mathbf{A}_{\text{map}}^{-CLS} = 0. \quad (6)$$

However, selecting negative categories requires careful consideration, as there are several viable strategies for identifying the most relevant examples. Below, we outline two

strategies that we applied in separate experiments to generate informative negatives:

LLM-Generated. We leverage a large language model to generate lists of visually similar subcategories for a given target class. These automatically identified sibling categories are then used to synthesize hard negatives. This approach produces highly targeted distractors and allows scalable, category-specific negative supervision. We used this strategy for most experiments.

Fine-vs-Broad. In this one-vs-many strategy, we synthesize images from a broad category while explicitly excluding the target subcategory. For example, if the target is *Canada Goose*, we generate images of *waterfowl* while negatively prompting the target class. This yields a diverse set of negative examples that may include visually similar distractors. We use this setup to ablate the effect of negative supervision.

4.2. Tuning the Specialization Module

To adapt the model to a novel fine-grained category at test time, we tune a specialization module that suppresses visually similar distractors and preserves the target object. This is achieved by using synthetic attention maps to optimize a subcategory-specific concept embedding, $z_{\text{concept}} \in \mathbb{R}^{512}$, which replaces the conditioning in a frozen open-

vocabulary segmentation network. We use CLIPSeg [20] for this purpose due to its accessibility. Because our goal is not precise segmentation but spatially-aware category specialization, we treat the coarse attention maps from synthetic exemplars as sufficient guidance for aligning the embedding with the visual concept of interest.

During tuning, we optimize this mask to match pseudo-labels extracted from synthetic exemplars. We use both positive and negative supervision to guide the embedding toward precise activation on the target category and away from visually similar but incorrect regions.

4.2.1 Positive Concept Alignment

To guide the concept embedding toward the target category, we first normalize each attention map to the range $[0, 1]$, and apply a fixed threshold of 0.5 to obtain a binary mask, \mathbf{A}_{bin} , that highlights the most salient regions for the category.

Each synthetic images x^{syn} is then preprocessed by the CLIP vision encoder to produce image features F^{syn} . We then pass both z_{concept} and F^{syn} to the CLIPSeg decoder, which outputs a predicted binary mask $\hat{\mathbf{A}}_{\text{pred}} \in [0, 1]^{H \times W}$. The concept embedding z_{concept} is optimized using a focal loss [16] between the predicted mask and the thresholded attention maps:

$$\mathcal{L}_{\text{neg}} = \text{FOCAL}(\hat{\mathbf{A}}_{\text{pred}}, \mathbf{A}_{\text{bin}}) \quad (7)$$

This encourages the concept embedding to activate in the correct spatial regions associated with the target category.

4.2.2 Negative Concept Loss

To discourage the concept embedding from activating on distractor regions or visually similar non-target objects, we introduce a negative concept loss. Given a set of synthetic images containing negative categories and their corresponding empty attention maps, we define the negative concept loss as:

$$\mathcal{L}_{\text{pos}} = \text{FOCAL}(\hat{\mathbf{A}}_{\text{pred}}, 0). \quad (8)$$

This penalizes false activations and improves the specificity of the concept embedding.

The total loss for tuning the Specialization module is the weighted sum of both components:

$$\mathcal{L}_{\text{concept}} = \mathcal{L}_{\text{pos}} + \lambda \mathcal{L}_{\text{neg}} \quad (9)$$

where λ controls the strength of negative supervision.

4.3. Specialization

After tuning the category-specific concept embedding, we apply the specialization module to refine the raw predictions of the class-agnostic counting model. Given a real

input image x and the tuned concept embedding z_{concept} , we pass both through the specialization module to produce a spatial mask $\hat{\mathbf{A}}_{\text{pred}}$ that represents the predicted relevance of each pixel to the target category. We then pass the image through the class-agnostic counter to produce D_{raw} , which may be either a density map or a point map. To suppress false positives, we re-weight the output using the predicted mask: $D_{\text{filtered}} = D_{\text{raw}} \odot \hat{\mathbf{A}}_{\text{pred}}$. This step preserves true positives while ignoring distractor regions, resulting in a category-specific output D_{filtered} that reflects only the target class.

5. Experiments

Implementation. To generate synthetic images, we use SDXL due to its strong performance in producing diverse fine-grained categories. All images are generated at a resolution of 768×768 , with 100 positive and 100 negative images per category, using 30 inference steps. For the specialization module, we use the pre-trained CLIPSeg model with ‘CIDAS/clipseg-rd64-refined’ weights. The category-specific concept embedding z_{concept} consists of 512 parameters and is initialized by encoding the category name using the CLIP text encoder. As our base counting model, we use PSeCo [33], a class-agnostic counter that tends to overcount in fine-grained scenarios—making it well suited for our specialization approach.

To tune z_{concept} , we first resize all synthetic images to 352×352 and extract image features using the CLIP vision encoder. We then optimize z_{concept} for 20 epochs using the AdamW optimizer [19] with a learning rate of 5×10^{-3} .

Evaluation Criteria. We evaluate all methods using mean absolute error (MAE), root mean squared error (RMSE), and relative absolute error (RAE). Because some subcategories contain more images than others, we normalize the evaluation to prevent any single subcategory from disproportionately influencing the overall result. Specifically, we first compute the average error for each subcategory by taking the mean over all images that contain it, and then average these values uniformly across all subcategories:

$$\text{Metric} = \frac{1}{C} \sum_{c=1}^C \left(\frac{1}{|I_c|} \sum_{i \in I_c} \mathcal{E}(y_i, \hat{y}_i) \right), \quad (10)$$

where C is the number of subcategories, I_c is the set of images containing subcategory c , $\mathcal{E}(y_i, \hat{y}_i)$ is the error metric.

Main Results. We evaluate our method on the LOOKA-LIKES dataset and compare it against several strong baselines. Since our approach requires only a user-specified text prompt to define the target category, we focus on two main

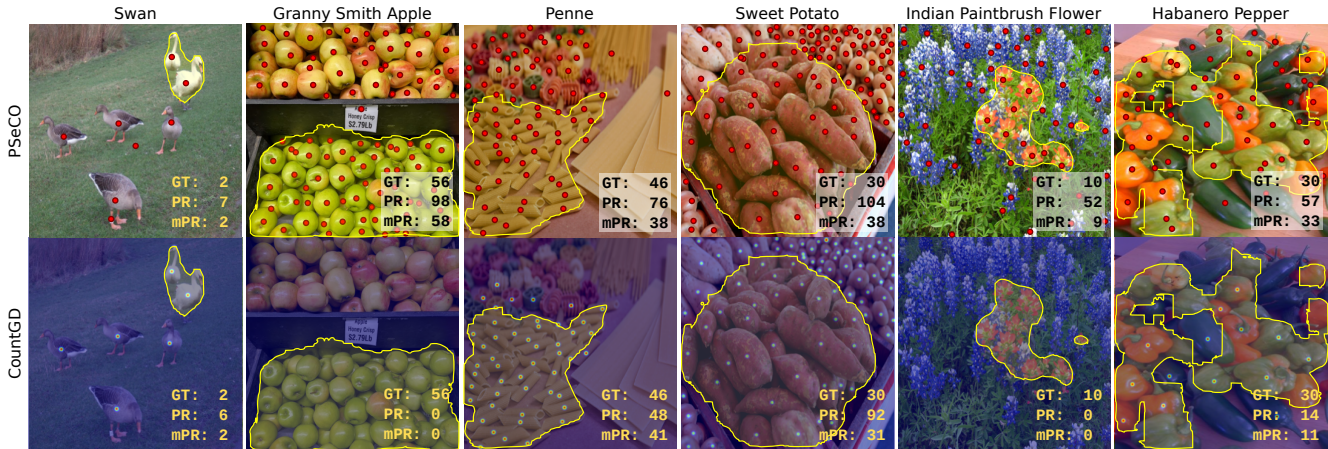


Figure 7. Qualitative results comparing PSeCo and CountGD on the LOOKALIKES dataset. Each image is evaluated using a fine-grained category prompt. The yellow mask indicates the output of our specialization network using the relevant concept embedding. While CountGD does not always overcount in fine-grained scenarios, it can be induced to do so by prompting for a broader category. *GT* denotes the truth count, *PR* is the predicted count, and *mPR* is the refined prediction from our method.

Method	Category Handling	Scope	Multi-Class	Real Data	MAE	RAE	MSE
OwlV2 [21]	Open-Vocab	Detect	✓	✓	37.25	3.02	55.01
Gr.Dino [18]	Open-Vocab	Detect	✓	✓	33.89	0.97	59.51
PseCo [33]	Text	Count	✗	✓	59.82	10.72	72.79
DAVE [23]	Text	Count	✗	✓	56.1	9.10	73.34
CountGD [1]	Text	Count	✗	✓	22.34	1.48	33.90
Ours + PseCo	Prompt Tune	Count	✗	✗	10.00	0.86	16.95

Table 2. Evaluation of counting and detection methods on the LOOKALIKES dataset. We use PseCo as the base counter.

Negative Source	MAE	RAE	MSE
No Negatives	20.90	2.01	34.3
Fine-vs-Broad	15.62	0.95	20.01
LLM-Generated	10.00	0.86	16.95

Table 3. We compare different approaches for selecting negative categories. LLM-generated hard negatives lead provide better suppression of irrelevant objects.

types of baselines: text-conditioned class-agnostic counting (CAC) methods, and open-vocabulary detection models. Together, these baselines represent a broad range of strategies for handling novel or fine-grained categories.

For CAC methods, we compare against PSeCo [33], DAVE [23], and CountGD [1]. For open-vocabulary detection, we include OWL-V2 [21] and GroundingDINO [18]. We also indicate whether training requires real data and whether a method is trained in a multi-class setting.

As shown in Table 2, our method outperforms all evaluated baselines on the LOOKALIKES dataset, highlighting the effectiveness of our prompt tuning strategy for category

Method	MAE	RAE	MSE
CLIPSeg	16.97	0.93	26.05
OVSeg	18.33	0.97	29.41
Ours	10.00	0.86	16.95

Table 4. Comparison to open-vocabulary segmentation methods. Each method uses PseCO.

specialization in challenging fine-grained object counting tasks.

Qualitative Analysis. Figure 7 presents qualitative results on several images from the LOOKALIKES dataset, highlighting the precision of our method and the failure modes of state-of-the-art class-agnostic counting approaches. We evaluate both CountGD and PSeCo using fine-grained category prompts, then apply our specialization method. PSeCo consistently overcounts across all examples and shows substantial improvement when refined by our method. CountGD performs slightly better when it can resolve the prompt but frequently fails to detect fine-grained

Method	Synth. Images	MAE	RAE	MSE
CountGD	-	22.35	1.48	33.90
Ours + PSeCo	10	14.78	1.20	23.25
Ours + PSeCo	25	13.98	1.17	22.64
Ours + PSeCo	50	11.74	1.10	20.02
Ours + PSeCo	100	10.00	0.86	16.95

Table 5. Impact of synthetic image count on performance. Each row reports the number of positive and negative images used to tune the concept vector.

categories altogether. Recent work have demonstrate that open-vocabulary methods, such as GroundingDINO, struggle substantially with fine-grained prompts [3]. CountGD is based on GroundingDINO and may inherent these limitations. However, our method can still be applied to CountGD in this setting by simply targeting a broader category.

We further highlight the first example (Swan) and the fifth example (Indian Paintbrush) in Figure 7. Both contain additional distractor objects—Greylag Geese and and Bluebonnets respectively—which were not part of the negative category image set during tuning of the concept embedding. These cases represent the robustness of our method to unseen categories at test time.

Influence of Synthetic Image Count In our main experiments, we identified image synthesis with SDXL as the primary source of computational cost in our pipeline. Since this cost scales linearly with the number of generated images, we evaluate whether comparable performance can be achieved with fewer synthetic examples.

Specifically, we assess the impact of reducing the number of synthetic images used to tune the concept vector in our specialization module. While our main results used 100 positive and 100 negative images per category, we additionally evaluate settings with 50, 25, and 10 positive/negative images. Results are reported in Table 5, and the perfor-

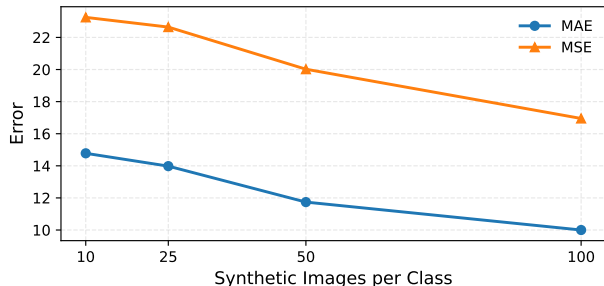


Figure 8. Many class-agnostic counting methods incorrectly count all visually similar objects.

mance trend is visualized in Figure 8.

We observe that even with only 50, 25, or even 10 images per category, our method still outperforms strong baselines such as CountGD by a substantial margin. These configurations represent approximately **50%**, **75%**, and **90%** reduction in computational cost, respectively, with only a marginal impact on performance. As shown in Figure 8, performance degrades gracefully as the number of synthetic images decreases, demonstrating the robustness of our approach under constrained resource settings.

5.1. The Impact of Irrelevant Objects

A key challenge in the LOOKALIKES dataset is distinguishing relevant from visually similar but irrelevant objects within the same image. To quantify this, we define the *Distractor Ratio*:

$$\text{Distractor Ratio} = \frac{C_{\text{irrel}} - C_{\text{rel}}}{C_{\text{rel}} + C_{\text{irrel}}} \quad (11)$$

where C_{rel} and C_{irrel} denote the counts of relevant and irrelevant objects, respectively. The ratio ranges from -1 (all relevant) to $+1$ (all irrelevant).

Fig. 9 plots Relative Absolute Error (rAE) versus Distractor Ratio using PSeCo as a baseline. As distractors increase, baseline error rises sharply due to false positives. In contrast, our method maintains stable performance. Even when irrelevant objects outnumber relevant ones (Distractor Ratio near $+1$), rAE remains nearly constant. This highlights the effectiveness of our filtering module in suppressing false positives and improving counting accuracy in cluttered, fine-grained scenarios.

Computational Cost. Our method introduces two main sources of computational overhead: synthetic image generation and prompt tuning. For each target category, we synthesize 100 positive and 100 negative images using SDXL at a resolution of 768×768 . On a single A100 GPU, this process takes approximately 5–7 minutes per category.

The second stage involves optimizing a 512-dimensional concept embedding for the specialization module using the synthetic data. This tuning step is lightweight, requiring 20 epochs and completing in under 30 seconds per category on a single V100 GPU. In total, the full test-time specialization process takes only 5-7 minutes per category and does not require the collection of any real data, making it practical for real-world applications where annotations are unavailable.

Negative Category Selection. Table 3 presents an ablation study comparing different strategies for negative category selection, as introduced in the methodology section. We also assess the effect of removing negative supervision entirely during tuning. This analysis reveals how different

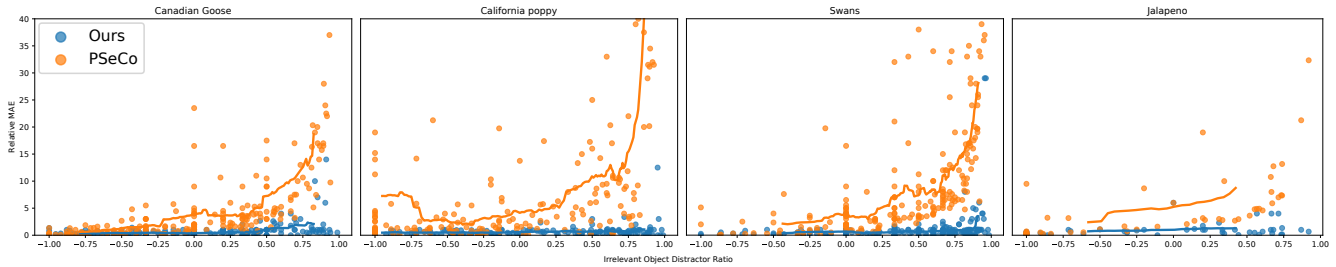


Figure 9. Our method (blue) drastically improves performance over PSeCo (orange) as the number of fine-grained distractor objects increases. Evaluated on a subset of the LOOKALIKES dataset.

negative sampling approaches influence the model’s ability to suppress visually similar distractors.

We observe that even without negative supervision, our method applied to PSeCO performs comparably to CountGD. The Fine-vs-Broad strategy yields reasonable performance but falls short of the LLM-Generated approach. This gap is primarily due to subcategories—such as cherry tomatoes and beefsteak tomatoes—where broad category exclusion is insufficient for precise specialization.

Comparison to Open-Vocabulary Segmentation. In Table 4, we compare our approach to the open-world segmentation methods OVSeg [15] and CLIPSeg [20]. Our method achieves significantly better performance on the LOOKALIKES dataset, underscoring the importance of our method for reducing false positives in fine-grained counting tasks. We attribute this improvement to the difficulty these open-vocabulary segmentation methods have in distinguishing between closely related subcategories, similar to those faced by class-agnostic counting models.

6. Conclusions

We present a simple yet powerful approach for fine-grained object counting. By leveraging synthetic data and tuning concept embeddings on the fly, our method transforms noisy overcounts into accurate, category-specific counts—without requiring real images or manual annotations.

Limitations. While effective on natural images, our method relies on the capacities of diffusion models. In domains with limited coverage, such as medical imaging, its applicability may be reduced. Future work could address this by incorporating methods like Break-A-Scene [2] to enable concept learning in underrepresented domains.

References

[1] N. Amini-Naieni, T. Han, and A. Zisserman. Countgd: Multi-modal open-world counting. In *Advances in Neural Information Processing Systems (NeurIPS)*, 2024. 7

[2] Omri Avrahami, Kfir Aberman, Ohad Fried, Daniel Cohen-Or, and Dani Lischinski. Break-a-scene: Extracting multiple concepts from a single image. In *SIGGRAPH Asia 2023 Conference Papers, SA ’23*, New York, NY, USA, 2023. Association for Computing Machinery. 9

[3] Lorenzo Bianchi, Fabio Carrara, Nicola Messina, Claudio Gennaro, and Fabrizio Falchi. The devil is in the fine-grained details: Evaluating open-vocabulary object detectors for fine-grained understanding. In *Proceedings of the IEEE/CVF Conference on Computer Vision and Pattern Recognition*, pages 22520–22529, 2024. 8

[4] Liu Chang, Zhong Yujie, Zisserman Andrew, and Xie Weidi. Countr: Transformer-based generalised visual counting. In *British Machine Vision Conference (BMVC)*, 2022. 2

[5] Xianing Chen, Si Huo, Borui Jiang, Hailin Hu, and Xinghao Chen. Single domain generalization for few-shot counting via universal representation matching. In *Proceedings of the Computer Vision and Pattern Recognition Conference*, pages 4639–4649, 2025. 1

[6] Siyang Dai, Jun Liu, and Ngai-Man Cheung. Referring expression counting. In *Proceedings of the IEEE/CVF Conference on Computer Vision and Pattern Recognition (CVPR)*, pages 16985–16995, June 2024. 3

[7] Adriano D’Alessandro, Ali Mahdavi-Amiri, and Ghassan Hamarneh. Afreeca: Annotation-free counting for all. In Aleš Leonardis, Elisa Ricci, Stefan Roth, Olga Russakovsky, Torsten Sattler, and Gül Varol, editors, *Computer Vision – ECCV 2024*, pages 75–91, Cham, 2025. Springer Nature Switzerland. 3

[8] Nikola Djukic, Alan Lukezic, Vitjan Zavrtanik, and Matej Kristan. A low-shot object counting network with iterative prototype adaptation, 2023. 2

[9] Adriano C. D’Alessandro, Ali Mahdavi-Amiri, and Ghassan Hamarneh. Learning-to-count by learning-to-rank. In *2023 20th Conference on Robots and Vision (CRV)*, pages 105–112, 2023. 3

[10] Shenjian Gong, Shanshan Zhang, Jian Yang, Dengxin Dai, and Bernt Schiele. Class-agnostic object counting robust to intraclass diversity. In Shai Avidan, Gabriel Brostow, Moustapha Cissé, Giovanni Maria Farinella, and Tal Hassner, editors, *Computer Vision – ECCV 2022*, pages 388–403, Cham, 2022. Springer Nature Switzerland. 1

[11] Ruifei He, Shuyang Sun, Xin Yu, Chuhui Xue, Wenqing Zhang, Philip Torr, Song Bai, and XIAOJUAN QI. Is syn-

- thetic data from generative models ready for image recognition? In *The Eleventh International Conference on Learning Representations (ICLR)*, 2023. 3
- [12] Menglin Jia, Luming Tang, Bor-Chun Chen, Claire Cardie, Serge Belongie, Bharath Hariharan, and Ser-Nam Lim. Visual prompt tuning. In *European Conference on Computer Vision (ECCV)*, 2022. 2, 3
- [13] Brian Lester, Rami Al-Rfou, and Noah Constant. The power of scale for parameter-efficient prompt tuning. In Marie-Francine Moens, Xuanjing Huang, Lucia Specia, and Scott Wen-tau Yih, editors, *Proceedings of the 2021 Conference on Empirical Methods in Natural Language Processing*, pages 3045–3059, Online and Punta Cana, Dominican Republic, Nov. 2021. Association for Computational Linguistics. 2, 3
- [14] Dingkang Liang, Jiahao Xie, Zhikang Zou, Xiaoqing Ye, Wei Xu, and Xiang Bai. Crowdclip: Unsupervised crowd counting via vision-language model. In *Proceedings of the IEEE/CVF Conference on Computer Vision and Pattern Recognition (CVPR)*, pages 2893–2903, June 2023. 3
- [15] F. Liang, B. Wu, X. Dai, K. Li, Y. Zhao, H. Zhang, P. Zhang, P. Vajda, and D. Marculescu. Open-vocabulary semantic segmentation with mask-adapted clip. In *CVPR*, 2023. 9
- [16] Tsung-Yi Lin, Priya Goyal, Ross Girshick, Kaiming He, and Piotr Dollar. Focal loss for dense object detection. In *Proceedings of the IEEE International Conference on Computer Vision (ICCV)*, Oct 2017. 6
- [17] Chang Liu, Henghui Ding, and Xudong Jiang. Gres: Generalized referring expression segmentation. In *Proceedings of the IEEE/CVF conference on computer vision and pattern recognition*, pages 23592–23601, 2023. 3
- [18] Shilong Liu, Zhaoyang Zeng, Tianhe Ren, Feng Li, Hao Zhang, Jie Yang, Chunyuan Li, Jianwei Yang, Hang Su, Jun Zhu, et al. Grounding dino: Marrying dino with grounded pre-training for open-set object detection. *Computer Vision – ECCV 2024*, 2024. 3, 7
- [19] Ilya Loshchilov and Frank Hutter. Decoupled weight decay regularization. In *International Conference on Learning Representations*, 2019. 6
- [20] Timo Lüddecke and Alexander Ecker. Image segmentation using text and image prompts. In *Proceedings of the IEEE/CVF Conference on Computer Vision and Pattern Recognition (CVPR)*, pages 7086–7096, June 2022. 6, 9
- [21] Matthias Minderer, Alexey Gritsenko, and Neil Houlsby. Scaling open-vocabulary object detection. *Advances in Neural Information Processing Systems*, 36, 2024. 7
- [22] Maria-Elena Nilsback and Andrew Zisserman. Automated flower classification over a large number of classes. In *2008 Sixth Indian conference on computer vision, graphics & image processing*, pages 722–729. IEEE, 2008. 3
- [23] Jer Pelhan, Alan Lukežič, Vitjan Zavrtnik, and Matej Kristan. Dave - a detect-and-verify paradigm for low-shot counting. In *Proceedings of the IEEE/CVF Conference on Computer Vision and Pattern Recognition (CVPR)*, pages 23293–23302, June 2024. 2, 3, 7
- [24] Dustin Podell, Zion English, Kyle Lacey, Andreas Blattmann, Tim Dockhorn, Jonas Müller, Joe Penna, and Robin Rombach. SDXL: Improving latent diffusion models for high-resolution image synthesis. In *The Twelfth International Conference on Learning Representations*, 2024. 4
- [25] Maan Qraitem, Kate Saenko, and Bryan A. Plummer. From fake to real: Pretraining on balanced synthetic images to prevent spurious correlations in image recognition. In Aleš Leonardis, Elisa Ricci, Stefan Roth, Olga Russakovsky, Torsten Sattler, and Gül Varol, editors, *Computer Vision – ECCV 2024*, pages 230–246, Cham, 2025. Springer Nature Switzerland. 3
- [26] Viresh Ranjan, Udbhav Sharma, Thu Nguyen, and Minh Hoai. Learning to count everything. In *Proceedings of the IEEE/CVF Conference on Computer Vision and Pattern Recognition (CVPR)*, 2021. 1, 2, 3
- [27] Deepak Babu Sam, Neeraj N Sajjan, Himanshu Maurya, and R Venkatesh Babu. Almost unsupervised learning for dense crowd counting. In *Proceedings of the AAAI Conference on Artificial Intelligence*, number 01, pages 8868–8875, 2019. 3
- [28] Jordan Shipard, Arnold Wiliem, Kien Nguyen Thanh, Wei Xiang, and Clinton Fookes. Diversity is definitely needed: Improving model-agnostic zero-shot classification via stable diffusion. In *Proceedings of the IEEE/CVF Conference on Computer Vision and Pattern Recognition*, pages 769–778, 2023. 3
- [29] Khoi Nguyen Thanh Nguyen, Chau Pham and Minh Hoai. Few-shot Object Counting and Detection. In *Proceedings of the European Conference on Computer Vision 2022*, 2022. 2
- [30] C. Wah, S. Branson, P. Welinder, P. Perona, and S. Belongie. Caltech-ucsd birds 200. Technical Report CNS-TR-2011-001, California Institute of Technology, 2011. 3
- [31] Chi Xie, Zhao Zhang, Yixuan Wu, Feng Zhu, Rui Zhao, and Shuang Liang. Described object detection: Liberating object detection with flexible expressions. *Advances in Neural Information Processing Systems*, 36, 2024. 3
- [32] Jingyi Xu, Hieu Le, Vu Nguyen, Viresh Ranjan, and Dimitris Samaras. Zero-shot object counting. In *Proceedings of the IEEE/CVF Conference on Computer Vision and Pattern Recognition*, pages 15548–15557, 2023. 2
- [33] Huang Zhizhong, Dai Mingliang, Zhang Yi, Zhang Junping, and Shan Hongming. Point, segment and count: A generalized framework for object counting. In *CVPR*, 2024. 2, 6, 7
- [34] Kaiyang Zhou, Jingkang Yang, Chen Change Loy, and Ziwei Liu. Conditional prompt learning for vision-language models. In *IEEE/CVF Conference on Computer Vision and Pattern Recognition (CVPR)*, 2022. 2, 3
- [35] Huilin Zhu, Jingling Yuan, Zhengwei Yang, Yu Guo, Zheng Wang, Xian Zhong, and Shengfeng He. Zero-shot object counting with good exemplars. In Aleš Leonardis, Elisa Ricci, Stefan Roth, Olga Russakovsky, Torsten Sattler, and Gül Varol, editors, *Computer Vision – ECCV 2024*, pages 368–385, Cham, 2025. Springer Nature Switzerland. 1, 2